Crystal Structure and Conformational Analysis of the Cognition Activator 5-Ethoxy-3-hydroxy-1-(phenylsulphonyl)pyrrolidin-2-one

Giuliano Bandoli,*[,a] Alessandro Dolmella,[a] Marino Nicolini,[a] Emilio Toja[b] and Francesco Tisato[c]
[a] Department of Pharmaceutical Sciences, University of Padua, Via F. Marzolo 5, I-35131 Padua, Italy
[b] ROUSSEL-PHARMA, V.le Gran Sasso 18, I-20131 Milano, Italy
[c] I.C.T.R.-C.N.R., Research Area, C.so Stati Uniti 4, I-35020 Camin-Padua, Italy

The preferred crystalline, solution and *in vacuo* arrangements of the title compound were investigated by means of single crystal X-ray diffraction, ^1H NMR spectroscopy and molecular mechanics calculations, respectively, and the findings were compared with those obtained for two similar compounds. The X-ray powder pattern diffraction was also collected.

This paper is intended to further develop our studies on the conformational properties of cognition activators and is also following shortly our last published paper.[1] Cognition activators are drugs currently employed for the symptomatic treatment of the pathological brain aging phenomena, which are usually referred to as Senile Cognitive Decline or Age Associated Memory Impairment;[2–6] in the light of the growing incidence of such illnesses among the older population, several families of compounds are being tested in laboratory and clinical trials. The nootropics (mind-targeted) family is the forerunner in the field,[5,7] and its key feature is the presence of the pyrrolidin-2-one ring. In this paper we evaluate the conformational preferences in the solid state, in solution and *in vacuo* of RU-47118 (I), the last member of the phenylsulphonyl

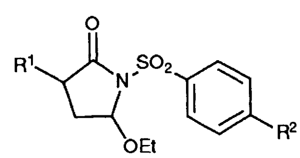

I; R^1 = OH, R^2 = H
II; R^1 = H, R^2 = H
III; R^1 = H, R^2 = NO_2

derivatives, kindly provided by Roussel-Uclaf. The interest in RU-47118 derives from the results of *in vivo* tests,[8] where it shows an anti-amnesic effect greater than the reference compound piracetam, and a potency greater than its analogues **II** and **III** in the scopolamine-induced amnesia test.[1,9,10] A comparison of the preferred arrangements assumed by compounds **I–III** was also undertaken.

Results and Discussion

Solid State.—The X-ray geometries and the crystal packing are shown in Figs. 1 and 2, together with the atomic numbering schemes. A list of atomic coordinates is given in Table 1.

The dihedral angle between the best mean planes of the five- and six-membered rings in **I** is 82.6°, and therefore in reasonable agreement with the values found in compound **II** [5-ethoxy-1-(phenylsulphonyl)pyrrolidin-2-one] and **III** [5-ethoxy-1-(4-nitrophenylsulphonyl)pyrrolidin-2-one], which are 70.8° and 104.5°, respectively.[11,12] The displacement of C(4) in the five-membered ring with respect to the N(1)–C(2)–C(3)–C(5) mean plane is 0.51 Å (compared to 0.43 Å in **II** and 0.47 Å in **III**), and takes place on different sides of the five-membered ring in **I**

Table 1 Final atomic coordinates ($\times 10^4$) with esds in parentheses

Atom	x	y	z
N(1)	3977(3)	195[a]	3020(1)
C(2)	4954(3)	699(3)	3845(2)
C(3)	3686(4)	247(3)	4728(2)
C(4)	1446(4)	−309(4)	4210(2)
C(5)	2011(4)	−1097(3)	3235(2)
S(6)	4844(1)	−155(2)	1881(1)
C(7)	4156(4)	1806(3)	1424(2)
C(8)	5686(4)	3057(4)	1549(2)
C(9)	5076(5)	4589(4)	1170(3)
C(10)	3012(5)	4838(4)	676(2)
C(11)	1505(5)	3586(4)	556(2)
C(12)	2066(4)	2064(3)	936(2)
O(13)	6450(3)	1649(3)	3837(2)
O(14)	3478(3)	1574(3)	5378(2)
O(15)	2584(3)	−2766(3)	3349(1)
C(16)	746(4)	−3837(4)	3078(3)
C(17)	1392(5)	−5534(4)	3365(3)
O(18)	7180(3)	−331(4)	1994(2)
O(19)	3460(3)	−1312(3)	1314(2)

[a] The y coordinate was fixed to define the origin along the twofold screw axis

compared with **II** and **III**. The pyrrolidine ring has then the typical half-chair (C_2, twist-envelope) conformation, which is the most usual situation in nootropics[11–15] (Fig. 1). From now on we will refer to the conformation of the five-membered ring in **I** as one with the 'flap up', and to that found in **II** and **III** as one with the 'flap down'. The superposition of the heavy-atom backbone, realised with the subroutine OFIT,[16] shows that the overall shape of the three compounds is similar. The fit is better when comparing **I** with **II** [r.m.s. deviation of 0.07 Å, largest deviation of 0.11 Å by O(13)], whereas the comparison of **I** with **III** [r.m.s. deviation of 0.16 Å, largest deviation of 0.28 Å by C(9)] is worse. The clearest difference when comparing **I** with **II** and **III** is in the arrangement assumed by the side-chain at C(5), where the O(15), though still occupying the axial position, is lying on the opposite side with respect to the five-membered ring; therefore, the side-chain in **I** is sampling a different region of space. The dihedral angles defining the side-chain at C(5) in **I** were also measured and compared with the corresponding ones in **II** and **III**. In **I** we found the C(4)–C(5)–O(15)–C(16) and C(5)–O(15)–C(16)–C(17) torsion angles to be 95.6° and −171.4°, respectively, while the corresponding values for **II** are −90.2° and 178.6°, and for **III** are −109.2° and 81.9°. According to the definition reported by Dale,[17] this angle sequence can be described as (+)anti-clinal/anti-periplanar in **I**, (−)anti-clinal/

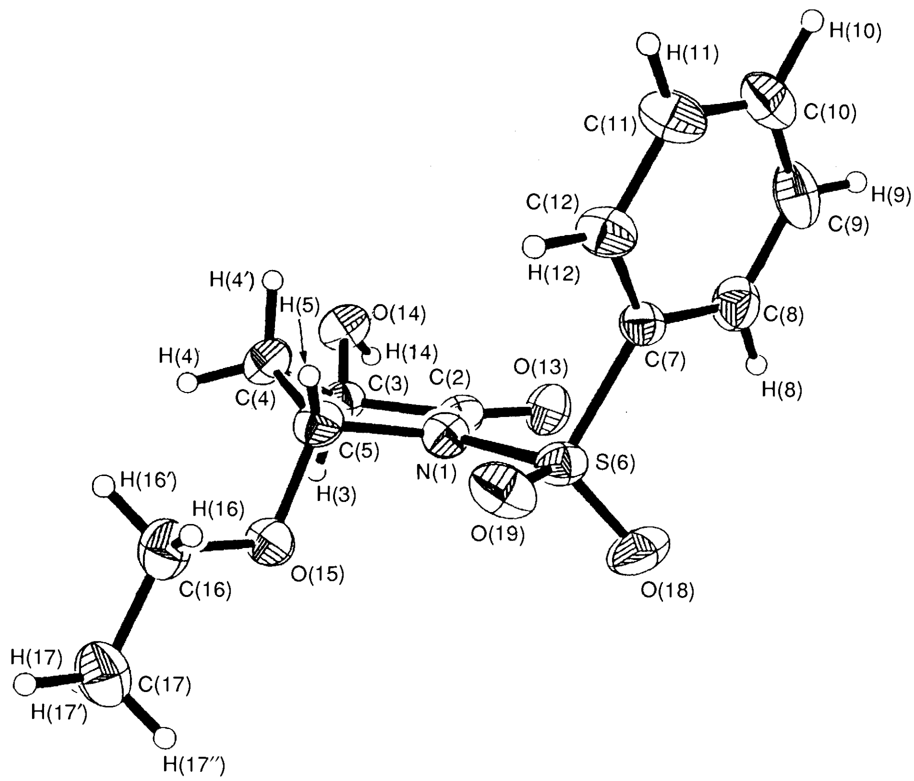

Fig. 1 ORTEP[30] representation of I with the atom-labelling scheme. Ellipsoids are scaled to enclose 30% of the electronic density.

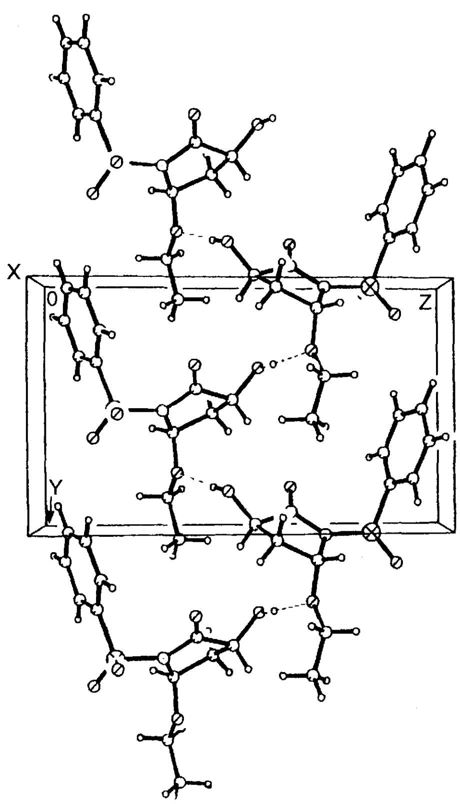

Fig. 2 Unit-cell packing of I, showing the hydrogen bond (dotted lines)

Table 2 Bond lengths/Å and angles/° with esds in parentheses

Bond	Length/Å	Bond angle	Angle/°
N(1)–C(2)	1.402(3)	C(2)–N(1)–C(5)	113.0(2)
N(1)–C(5)	1.456(3)	C(2)–N(1)–S(6)	124.4(1)
N(1)–S(6)	1.671(2)	C(5)–N(1)–S(6)	122.4(1)
C(2)–C(3)	1.527(4)	N(1)–C(2)–C(3)	106.4(2)
C(2)–O(13)	1.194(3)	N(1)–C(2)–O(13)	125.9(2)
C(3)–C(4)	1.523(3)	C(3)–C(2)–O(13)	127.6(2)
C(3)–O(14)	1.408(4)	C(2)–C(3)–C(4)	102.5(2)
C(4)–C(5)	1.532(4)	C(2)–C(3)–O(14)	112.4(2)
C(5)–O(15)	1.413(4)	C(4)–C(3)–O(14)	112.2(2)
S(6)–C(7)	1.752(3)	C(3)–C(4)–C(5)	104.1(2)
S(6)–O(18)	1.413(2)	N(1)–C(5)–C(4)	102.7(2)
S(6)–O(19)	1.427(2)	N(1)–C(5)–O(15)	108.4(2)
C(7)–C(8)	1.378(4)	C(4)–C(5)–O(15)	112.9(2)
C(7)–C(12)	1.375(3)	N(1)–S(6)–C(7)	104.6(1)
C(8)–C(9)	1.388(5)	N(1)–S(6)–O(18)	108.1(1)
C(9)–C(10)	1.364(4)	C(7)–S(6)–O(18)	109.1(2)
C(10)–C(11)	1.369(4)	N(1)–S(6)–O(19)	104.5(1)
C(11)–C(12)	1.373(4)	C(7)–S(6)–O(19)	108.5(1)
O(15)–C(16)	1.431(3)	O(18)–S(6)–O(19)	120.8(2)
C(16)–C(17)	1.482(5)	S(6)–C(7)–C(8)	120.5(2)
		S(6)–C(7)–C(12)	118.6(2)
		C(8)–C(7)–C(12)	121.0(3)
		C(7)–C(8)–C(9)	118.6(2)
		C(8)–C(9)–C(10)	120.3(3)
		C(9)–C(10)–C(11)	120.6(3)
		C(10)–C(11)–C(12)	120.0(3)
		C(7)–C(12)–C(11)	119.5(3)
		C(5)–O(15)–C(16)	112.9(2)
		O(15)–C(16)–C(17)	109.4(2)

anti-periplanar in **II** and (−)anti-clinal/(+)syn-clinal in **III**; therefore, we may say that there is a good agreement in the preferred orientation of the side-chain when comparing **I** with **II**, whereas the comparison of **I** with **III** shows significant differences. The bond lengths and angles (Table 2) are within the expected values and do not merit any special comment, while a well-defined intermolecular hydrogen bond, a feature completely absent in **II** and **III**,[11,12] is found in compound **I**. The interaction involves the O(14)–H(14) hydroxy group and the O(15) ether oxygen [O(14)–H(14)···O(15) 174.5°; O(14)···O(15) 2.83 Å] (Fig. 2). The unit cell parameters and atomic coordinates obtained from the single-crystal

Table 3 ^1H NMR spectral parameters of **I** (multiplicity shown in parentheses) in $C_6D_6/CDCl_3$ (7:3) solution and calculated[a] coupling constant values (J_{calc}, Hz) for vicinal protons of A and B conformers of the pyrrolidin-2-one moiety derived from optimized torsion angles (°) through force field calculations

				Conformation			
				A (flap up)		B (flap down)	
Proton[b]	δ(ppm)	J/Hz		J_{calc}[c]	Torsion angle[d]	J_{calc}[c]	Torsion angle[d]
H(3)	4.04 (ddd)	$J_{3,14}$	3.43				
H(4)	1.92 (dd)	$J_{3,4}$	7.61	7.8	−35.5	5.6	34.1
H(4′)	1.43 (ddd)	$J_{3,4'}$	10.43	9.0	−154.9	1.3	−85.6
H(5)	5.14 (d)	$J_{4,4'}$	12.56				
H(14)	2.05 (d)	$J_{4,5}$	−0.02	1.4	−88.6	9.2	−157.4
H(16)	3.51 (dq)	$J_{4',5}$	5.45	6.0	31.8	7.0	−36.2
H(16′)	3.22 (dq)	$J_{16,16'}$	9.19				
Me(17)[e]	0.95 (t)	$J_{16,17}$	6.99				
		$J_{16',17}$	6.99				
H(8–12)	6.97 (m)[f] 8.03 (m)[f]						

[a] The calculated probable errors resulting from the fitting are less than 0.03 for all parameters. [b] ^1H (multiplicity shown in parentheses) NMR chemical shifts in $CDCl_3$ solution: H(3) 4.59; H(4) 2.54; H(4′) 2.05; H(5) 5.60; H(14) 2.77; H(16) 3.81; H(16′) 3.67; Me(17) 1.24; H(8–12) 7.63, 8.05 ppm; C(2) 174.05 (s); C(3) 68.67 (d); C(4) 36.46 (t); C(5) 86.41 (d); C(16) 65.13 (t); C(17) 15.02 (q); C(7) 138.12 (s); C(8,12) 128.90 (dd); C(9,11) 128.42 (dt); C(10) 134.25 (dt) ppm. [c] From extended Karplus equation.[21] [d] Calculated by molecular mechanics.[18] (MM2) [e] Chemical shifts of hydrogen atoms bonded to C(17). [f] Unresolved multiplets.

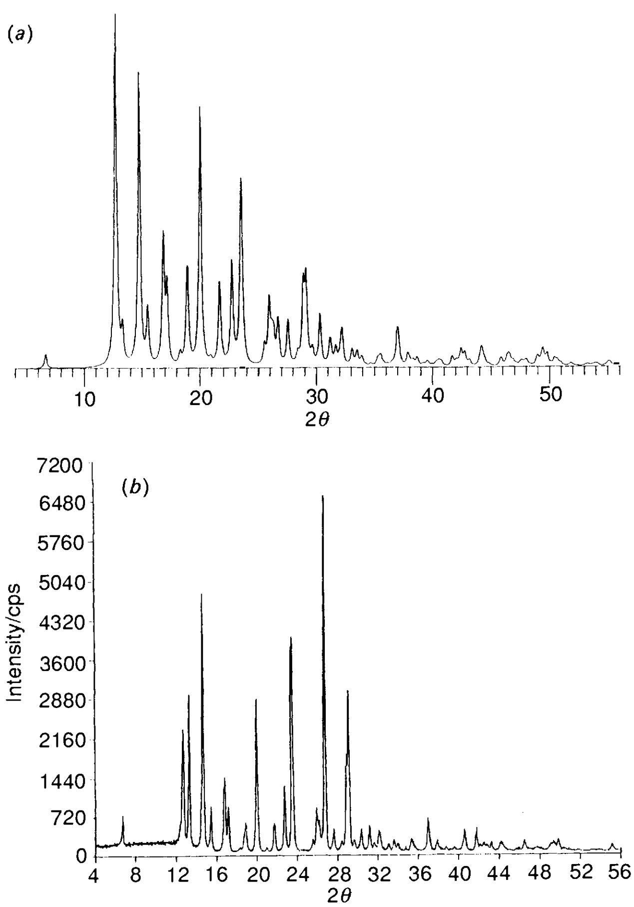

Fig. 3 (*a*) Computer-generated powder pattern; (*b*) experimental powder pattern.

structure analysis were employed to calculate a predicted powder pattern using the subroutine XPOW,[16] and the simulated/experimental powder diffraction patterns are presented in Fig. 3. The comparison suggests that the single crystal is a good representative of the commercial RU-47118 powder sample.

^1H *NMR Spectroscopy*.—Proton signals of the pyrrolidin-2-one ring are easily assigned looking at the two-dimensional map. The only relevant feature is the different multiplicities showed by H(4) and H(4′), due to the fact that the dihedral angle between the H(5)–C(5)–C(4) and H(4)–C(4)–C(5) planes is close to 90°, as found in the solid state and by molecular mechanics [18] calculations. According to previously reported data for nootropics,[11,12,19] a pair of conformers, having the C(4) displaced 'at the flap' on opposite sides in respect of the C(2)–C(3)–C(5)–N(1) mean plane, are possible for **I**; these are indicated as A (flap up, as found in the crystal structure), and B (flap down). Theoretical calculations performed on the A and B arrangements using the Karplus relationship[20] for vicinal proton–proton coupling constants and a generalized Karplus equation[21] for the optimized H–C–C–H dihedrals show a good agreement for the measured (J_{exp}) and calculated (J_{calc}) coupling constant values for the A conformation (flap up) (Table 3).

Calculations.—Molecular mechanics (MM) calculations[22] were performed to elucidate the preferred *in vacuo* arrangement of **I**, and a conformational energy map was prepared following the scheme formerly employed in a series of semiempirical quantum mechanical calculations.[1,12] The optimized X-ray geometry was chosen as the starting point for all subsequent calculations, and the ω_1 and ω_2 torsion angles [C(2)–N(1)–S(6)–C(7) and N(1)–S(6)–C(7)–C(8), respectively] were driven with a step of 10° in the 360° space, allowing for relaxation at each step. Of the two possible envelope arrangements (see above) only the one presented in the solid state (flap up) was retained in the calculations. Eight minima, corresponding to four distinct molecular arrangements, were identified, in complete agreement with the results obtained for **II** and **III**[23] (Fig. 4).

The discussion is limited to the positive values of ω_2, since the rotation about this torsion angle shows a symmetrical behaviour (periodicity of π). The minima are found at ω_1, ω_2 values of: −160.7°, 70.2° (**1**); −79.3°, 89.8° (**2**); 79.4°, 100.0° (**3**); 160.1°, 100.1° (**4**); of these, minimum **3** is the lowest, with minima **1**, **2** and **4** within 1 kcal mol^{-1} mol above it.* The general

* 1 cal = 4.184 J.

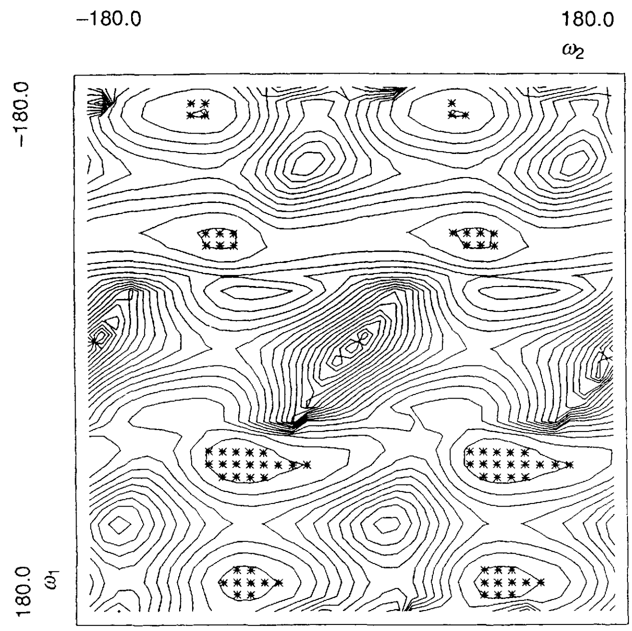

Fig. 4 Contour map of calculated conformational energies of **I** as a function of the rotational angles ω_1 and ω_2. Energy range from 0 to 20 kcal mol^{-1} (relative to the minimum), contoured lines drawn at 1 kcal mol^{-1} intervals. The starred points indicate the low-energy areas of the map.

appearance of the potential energy map, as well as the distribution and position of the minima, look similar for compounds **II** and **III**,[23] but the calculations find the lowest energy conformation in the negative domain of ω_1. Similar results are obtained with MOPAC[24] calculations, where the lowest energy conformations are in the negative domain of ω_1 for compounds **II** and **III**,[12] and for **I** the most stable conformer takes the $\omega_1 = \omega_2$ value of $+72°$.[23] The interconversion between minima **2** and **3** in **I** is hampered by a rotational barrier close to 7 kcal mol^{-1}; similarly, the migration between minima **1** and **2** is hindered by another barrier of *ca.* 5 kcal mol^{-1}, and that between minima **3** and **4** by yet another one of *ca.* 3.5 kcal mol^{-1}. We point out here that the adopted scheme did not give us the opportunity of directly evaluating the error associated with the calculations, and therefore the figures quoted above have to be taken with a bit of caution. The first barrier, according to previous reports,[12] should prevent the molecule from moving between the minima, while the second, and especially the third, should allow more freedom and the existence of the involved arrangements, with minimum **3** being the preferred one. No attempt was made of characterizing the transition structures associated with the migration between minima; instead, another series of calculations was undertaken to better characterize the minima **1**–**4** mentioned above. The input geometry was, in this case, that resulting from the optimization of the calculated coordinates of minima **1**–**4**. The torsion angles leading the motion of the C(5) side-chain, ω_3 and ω_4 [C(4)–C(5)–O(15)–C(16) and C(5)–O(15)–C(16)–C(17), respectively], were then driven in the 360° space with the scheme formerly employed for ω_1 and ω_2, while restraining the same angles to the initial positions. Only the lowest energy conformation found in each calculation was retained and underwent a final optimization. The final geometries were then compared with the X-ray geometry of **I** and with the X-ray, *in vacuo*[12,23] preferred arrangements of **II** and **III**, considering the ω_1, ω_2, ω_3 and ω_4 torsion angles (Table 4). Such comparison suggests a few remarks. Both MM and MOPAC succeed in locating the X-ray arrangement as a low-energy conformation, and the calculations' results are shown to be consistent along the series **I**–**III**. In particular, MM always finds ω_3, ω_4 in compounds **I**–**III** lying close to $\pm 90°$, $\pm 180°$, respectively, (clinal-anti orientation[17]), as well as very close to the corresponding experimental (X-ray) values. The clearest difference between compound **I** and compounds **II** and **III** (looking at the dihedral angle values) is that the preferred *in vacuo* conformation does not fall in the negative domain of ω_1, as expected from X-ray and MOPAC calculations.[12] In this respect there is a better agreement between minimum **2** of **I** and the X-ray geometry, as well as between minimum **2** of **I** and the calculated[23] lowest energy arrangements of **II** and **III**; still, the calculated MM lowest energy arrangements for **I**, **II**, **III**, look similar for showing the C(5) side-chain and the phenyl ring on the same side of the pyrrolidine moiety, *i.e.* opposite to the flap. Comparison of MM and MOPAC results gives the feeling that MM better reproduces the experimental data, again when considering minimum **2** of **I** and the calculated[12,23] lowest energy arrangements for **II** and **III**. MM calculations, furthermore, always locate a larger number of minima than MOPAC calculations, proving to be a better system for the exploration of the conformational surfaces than semiempirical methods.

Conclusions

The preferred solid state solution and *in vacuo* arrangements of **I** were analysed and compared with those of similar compounds **II** and **III**. The solid-state data show that there is no relevant difference in the reciprocal position of the five- and six-membered rings, but the position of the C(5) side-chain in **I**, as well as that of C(4) in the five-membered ring mirrors that assumed in compounds **II** and **III**. The analysis of **I** in solution gives an arrangement which is in agreement with the solid state results, while the computational analysis locates three more possible conformations, all of which are within 1 kcal mol^{-1} of the lowest energy conformation. The solid state arrangement corresponds to minimum **2** for **I**, with minimum **3**, the lowest energy conformer in MM calculations, *ca.* 1 kcal mol^{-1} below **2**. All minima (in all compounds) present a clinal-anti orientation of the C(5) side-chain which is also very similar to the experimental (X-ray) data; besides, in the lowest energy arrangements of all compounds, we consistently find the phenyl ring and the C(5) side-chain on the same side (opposite to the flap) of the pyrrolidine moiety. All the low-energy arrangements, following the examination of the rotational barriers between them, seems to coexist in the gas phase, and the comparison of the MM and MOPAC calculated structures for compounds **I**–**III** indicates that the solid state arrangement can be preserved *in vacuo*. From what has been said above, it is very hard to draw a definitive conclusion about the major biological activity recorded for **I** in respect of similar compounds **II** and **III** on conformational grounds, since the general molecular structure is preserved, with the exception of the C(5) side-chain. The presence of two nucleophilic sites [the oxygens at C(3) and C(5)] at both sides of the five-membered ring might be relevant on electronic grounds, because it might be responsible for a better positioning and/or binding to the receptor site. Additional studies on this last hypothesis need to be carried out to better elucidate the problem.

Experimental

X-Ray Work.—Single crystal diffraction. A white transparent crystal formed by slow evaporation of a propan-2-ol solution, of dimensions *ca.* 0.2 × 0.3 × 0.1 mm was used.

Crystal data. $C_{12}H_{15}NO_5S$, M = 285.3, monoclinic, a = 6.053(1), b = 8.183(2), c = 13.426(3) Å, β = 96.32(2)°, V =

Table 4 Comparison of experimental (X-ray) and theoretical (MM, MOPAC) conformations of **I–III**. Dihedral angles/°.

	I					**II**[a]			**III**[a]		
Angle	Exp.	**1**	**2**	**3**	**4**	Exp.	MM[23]	MOPAC[12]	Exp.	MM[23]	MOPAC[12]
ω_1	−69.5	−164.0	−76.1	76.2	160.9	−68.8	−76.2	−66.2	−69.8	−76.8	−65.0
ω_2	93.4	73.9	86.3	99.3	101.5	89.6	77.6	106.9	81.1	77.4	104.3
ω_3	95.6	91.4	91.8	93.0	95.8	−90.2	−93.0	−127.3	−109.2	−93.1	−124.8
ω_4	−171.4	177.0	−178.6	−177.1	175.8	−178.6	177.1	−156.3	81.9	177.1	−154.4

[a] Only the lowest energy conformer found by molecular mechanics reported.

660.9(3) Å^3, space group $P2_1$, $Z = 2$, $D_c = 1.434$, $D_x = 1.43(1)$ g cm^{-3}, $\mu = 2.5$ cm^{-1}. The lattice parameters were obtained from least-squares analysis of 50 reflections with $2\theta > 25°$, from graphite monochromated Mo-Kα radiation ($\lambda = 0.71073$ Å) on a Siemens Nicolet R3m/V diffractometer. Intensity data of 1628 unique reflections were collected at room temperature by $\omega - 2\theta$ scan technique with 2θ between 4 and 55° and $-7 < h < 7$, $0 < k < 10$, $0 < l < 17$. Intensity and orientation of two standard reflections were measured again every 100 reflections; no significant decomposition or movement of the crystal was observed. Corrections were made for Lorentz and absorption effects. The systematic absences ($0k0$ absent if $k = 2n + 1$) allow the space group to be either $P2_1$ or $P2_1/m$. With $Z = 2$, the latter would require the molecule to have either mirror or inversion symmetry and this was unlikely. $P2_1$ was chosen and confirmed by the analysis. The structure was solved by direct methods.[16] All of the non-hydrogen atoms came out from the E maps with the highest figure of merit, while all of the hydrogens appeared on difference electron density maps after refinements. However, all hydrogen atoms were fixed at calculated positions (with C–H = 0.96 Å, O–H = 0.85 Å and U = 0.08 Å^2). The final R, R_w values are 0.034 and 0.042 for the 1444 unique reflections [$|F_o| > 3\sigma|F_o|$]. A weighting scheme is $w = [\sigma^2|F_o| + 0.0005|F_o|^2]^{-1}$ and the quantity minimized in full-matrix least-squares refinement is $\Sigma w|F_o| - |F_c|)^2$. In the final ΔF map the largest peak is 0.25 eÅ^{-3}, the largest hole −0.22 eÅ^{-3}. The atomic scattering factors were taken from International Tables for X-ray Crystallography.[25] Differentiation between enantiomorphs, as expected, could not be made on the basis of the X-ray results. The final non-hydrogen atomic coordinates with their estimated standard deviations are given in Table 1. The bond distances and angles are shown in Table 2. Supplementary material has been deposited at the Cambridge Crystallographic Data Centre (CCDC).*

Powder Pattern Diffraction.—The X-ray powder diffraction data of the commercial RU-47118 sample were collected using an automated Siemens D500 Kristalloflex diffractometer. The instrument set up was 40 kV/30 mA, and the experiment was performed in a continuous scan mode, with a scanning rate of 0.5° min^{-1} of 2θ (2θ max = 56°, Cu-Kα_1 wavelength = 1.540 59 Å). We employed the Bragg-Brentano focussing geometry, with an incident aperture of 1° of divergence, and monochromator and detector apertures of 0.018° and 0.015°, respectively. The raw diffraction data were stripped of background, smoothed and searched for diffraction maxima using the Siemens DIFFRAC500 (V1.1A) Powder Diffraction Evaluation Software Package (1988). The intensities of the diffraction lines were measured as peak heights above background and expressed in percentage of the strongest line (see Supplementary material). The unit cell parameters were calculated, then refined and the reflections indexed using 28 of the best resolved peaks, and the least-squares refinement program[26] supplied as part of the Siemens Software package. The refined lattice constants from powder were: $a = 6.06$, $b = 8.17$, $c = 13.41$ Å, $\beta = 96.35°$; the $2\theta_{obs} - 2\theta_{calc}$ values never exceeded $\pm 0.03°$ (except the 001 and 002 reflections), with $F_{28} = 100\,(0.01, 94)$.[27]

^{1}H *NMR Spectroscopy*.—The proton NMR spectra of the title compound were obtained on a Bruker AC-200 spectrometer operating at 200.133 MHz and a probe temperature of 293 K. A sample of RU-47118 was dissolved in $C_6D_6/CDCl_3$ (7/3, *ca.* 10 µmol dm^{-1}) and the chemical shifts were measured relative to tetramethylsilane = 0.0 ppm as internal standard. The assignments of the aliphatic proton resonances can be unambiguously made from the relative integrations, spin–spin splittings, and bi-dimensional homonuclear shift correlation (COSY) experiments.[28] The proton spectra were analysed by computer simulation on an ASPECT-2000 Bruker computer, using the Bruker PANIC iterative program, and the refined scalar coupling constants were reported in Table 3. Theoretical J values for related torsion angles of vicinal protons were calculated through a generalized Karplus equation[21] using the MacroMODEL program,[18] which employed the MM2 force field.

Conformational Analysis.—Molecular mechanics calculations[22] were performed on a Silicon Graphics IRIS-4D 320 VGX workstation (IRIX version 3.0) by means of the Biosym's INSIGHT II (version 2.0.0) and DISCOVER (version 2.7.0) program packages,[29] and the *in vacuo* preferred arrangement of **I** was analysed. The optimized X-ray geometry was used as the starting point for subsequent calculations; the relaxation of the crystallographic coordinates was achieved with the DISCOVER minimization routine until the maximum absolute derivative (mad) of the molecular energy dropped below 0.001 kcal mol^{-1} Å^{-1} (100 steps of steepest descent + 100 steps of conjugate gradients + 100 steps of the VA09A minimizer algorithms). Only the solid-state-like envelope arrangement of the five-membered ring (flap up) was retained. A conformational energy map was generated by driving the ω_1 and ω_2 dihedrals [C(7)–S(6)–N(1)–C(2) and C(8)–C(7)–S(6)–N(1), respectively], in the 360° space with a step of 10°. The structure was minimized at each step (mad < 0.0001), but the ω_1 and ω_2 angles were restrained to the driven values (TorsionForce routine in DISCOVER[29]). Eight minima, corresponding to four distinct arrangements, were identified. Each low-energy conformation was further minimized (mad < 0.000 01) and the geometries obtained were used in another series of calculations, where the torsion angles responsible for the C(5) side-chain motion [ω_3, ω_4; C(4)–C(5)–O(15)–C(16) and C(5)–O(15)–C(16)–C(17), respectively] were driven in the 360° space as above described. Relaxation was still allowed at each step (mad < 0.0001), but the ω_1, ω_2 values were restrained to those of the previously optimized minima (Tether routine in DISCOVER[29]). The lowest energy conformation found in each new calculation was again optimized (mad < 0.000 01) and taken as the fully relaxed arrangement for each of the first four minima.

* For details of the deposition scheme, see Instruction for Authors, *J. Chem. Soc., Perkin Trans. 2*, 1991, issue 1.

References

1 G. Bandoli, A. Dolmella, M. Nicolini and E. Toja, *Cryst. Spectr. Res.*, 1991, in the press.
2 T. Crook, *Psychopharmacol. Bull.*, 1988, **24**, 31.
3 W. H. Moos, R. E. Davis, R. D. Schwarz and E. R. Gamzu, *Med. Res. Rev.*, 1988, **8**, 353.
4 E. R. Gamzu, T. M. Hoover, S. I. Gracon and M. V. Ninteman, *Drug Development Res.*, 1989, **18**, 177.
5 W. H. Moos and F. M. Hershenson, *Drug News and Perspectives*, 1989, **2**, 397.
6 W. E. Muller, *Drug News and Perspectives*, 1989, **2**, 295.
7 C. E. Giurgea, *Drug Development Res.*, 1982, **2**, 441.
8 E. Toja, C. Gorini, F. Barzaghi and G. Galliani, Eur. Pat. 294295, 1988; *Annual Drug Data Report*, 1989, **11**, 450.
9 E. Toja, C. Gorini, C. Zirotti, F. Barzaghi and G. Galliani, Eur.Pat. 229566, 1987; *Annual Drug Data Report*, 1988, **10**, 97.
10 E. Toja, C. Gorini, C. Zirotti, F. Barzaghi and G. Galliani, *Eur. J. Med. Chem.*, 1991, **26**, 403.
11 M. E. Amato, G. Bandoli, U. Casellato, G. C. Pappalardo and E. Toja, *J. Mol. Struct.*, 1990, **238**, 413.
12 M. E. Amato, G. Bandoli, A. Dolmella, A. Grassi, G. C. Pappalardo and E. Toja, *J. Mol. Struct.*, 1991, **245**, 81.
13 G. Bandoli, A. Grassi, M. Nicolini and G. C. Pappalardo, *Chem. Pharm. Bull.*, 1985, **33**, 4395.
14 G. Bandoli, M. Nicolini, G. C. Pappalardo, A. Grassi and B. Perly, *J. Mol. Struct.*, 1987, **157**, 311.
15 G. Bandoli, M. Nicolini, H. Lumbroso, A. Grassi and G. C. Pappalardo, *J. Mol. Struct.*, 1987, **160**, 297.
16 G. M. Sheldrick, SHELXTL-PLUS: An Integrated System for Solving, Refining and Displaying Crystal Structures from Diffraction Data. For Nicolet R3m/V. University of Göttingen, Germany, 1987.
17 J. Dale, *Stereochemistry and conformational analysis*, Verlag Chemie, New York, Weinheim, 1978, p. 487.
18 F. Mohamadi, N. G. J. Richards, W. C. Guida, R. Liskamp, M. Lipton, C. Canfield, G. Chang, T. Hendrickson and W. C. Still, *J. Comput. Chem.*, 1990, **11**, 440.
19 M. E. Amato, G. Bandoli, F. Djedaïni, A. Dolmella, A. Grassi and G. C. Pappalardo, *J. Mol. Struct.*, 1990, **222**, 487.
20 M. Karplus, *J. Chem. Phys.*, 1959, **30**, 11.
21 C. A. G. Haasnot, F. A. A. M. De Leeuw and C. Altona, *Tetrahedron*, 1980, **36**, 2783.
22 U. Burkert and N. L. Allinger, *Molecular mechanics*, American Chemical Society, Monograph 177, Washington D. C., 1982.
23 G. Bandoli and A. Dolmella, unpublished work.
24 J. J. P. Steward, *J. Computer-Aided Mol. Design*, 1990, **4**, 1 and MOPAC Manual (Fifth Ed.). A General Molecular Orbital Package.
25 *International Tables for X-ray Crystallography*, Kynoch Press, Birmingham, 1974, vol. IV, pp. 202–207.
26 D. E. Appleman and H. T. Evans Jr., U.S. Geological Survey, Computer Contribution 20, U.S. National Technical Information Service, Document PB 2-16188, 1973.
27 G. S. Smith and R. L. Snyder, *J. Appl. Cryst.*, 1979, **12**, 60.
28 W. Peters, M. Fuchs, H. Sicius and W. Kuchen, *Angew. Chem., Int. Ed. Engl.*, 1985, **25**, 231.
29 Biosym Technologies, Inc., 10065 Barnes Canyon Road, San Diego, CA 92121.
30 C. K. Johnson, ORTEPIL Report ORNL-5138. Oak Ridge National Laboratory Tennessee, 1976, Tennessee, U.S.A.

Paper 1/04544J
Received 2nd September 1991
Accepted 25th September 1991